A Revolution in Lighting:

Building the Science and Technology Base

for Ultra-Efficient Solid State Lighting

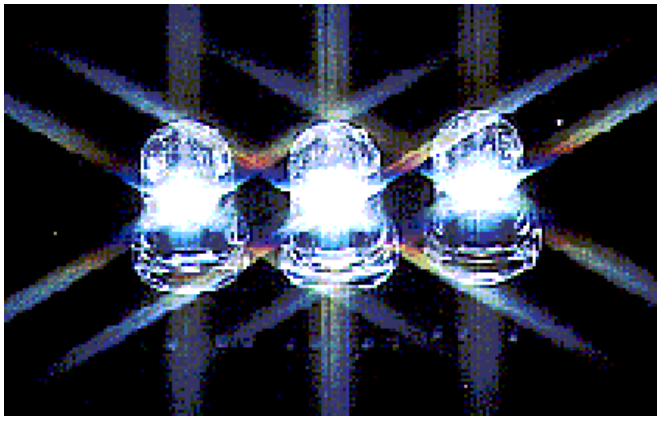

FY02 2nd Year Renewal

- Advancing the Science and Technology of Materials and Reactors
- Pushing the Envelope on LED and VCSEL Efficiency and Color
- Developing the Smart Luminaire

INTRODUCTION

Overview

The opportunities for Sandia National Laboratories and DOE in solid-state lighting and in the important GaN material system are very large. The market for high-brightness LEDs grew by nearly 58% last year and achieved worldwide revenues of around $1.2B. We have already begun technical collaborations with two of the solid-state lighting companies, submitted a joint proposal to DOE/BTS with one company, and are fielding requests for collaboration from other companies. The Optoelectronics Industry Development Association is continuing to promote interest in a National Initiative in Solid-State Lighting on behalf of the solid-state lighting companies – including sponsorship with the National Research Council of a workshop on solid-state lighting at the National Academy of Sciences. While the priorities in the first budget submission from the new Administration has not favored energy efficiency research, we believe that the initiative will eventually receive favorable attention due to the increased awareness of an "energy crisis". The opportunity of solid-state lighting (10X and 2X improvement in efficiency compared to incandescent and fluorescent lamps, respectively) for energy reduction is simply too important to pass.

Growth in National Security Synergies

Meanwhile, there is significant interest in the III-nitride material system for various national security-related projects in DARPA, Office of Naval Research, and Sandia's non-proliferation and weapons programs due to some of the unique properties of GaN and related alloys. Our project is strongly coupled with Sandia's GaN electronics initiative. For example, defect reduction using cantilever epitaxy is a key driver for both programs while some Sandia non-proliferation programs have a strong interest in our UV emitters.

Our program has also made excellent use of other Sandia initiatives. For example, the reactor design work is very computationally intensive. We are using modeling and simulation codes developed within the ASCI and related programs. Similarly, our work in photonic lattices may be able to use the EUVL lithography tools while the GaN material characterization and CVD chemistry tasks are strongly coupled with on-going BES projects.

External Advisory Committee Review

An External Advisory Committee reviewed the project in February. The External Advisory Committee consisted of some of the most respected senior researchers from solid-state lighting companies, academia, and lighting research. (Please see Appendix for EAC report and membership.) The EAC gave a strong recommendation to the project, including the following:

> *"your [Sandia's] program goals are very important and appropriate to your … inherent strengths. Your breadth of expertise within the Labs allows you to bring together the many different disciplines that are needed to address the complex issues that need to be solved. You have a very strong team working on this LDRD. However, we feel that*

you need increased resources to accomplish your Tasks' objectives. … We also recommend that you create a better integration of focus among the varying Tasks."

Summary of Accomplishments

While we are early in the project still, our progress to date gives us confidence that the project will have a significant impact on solid-state lighting and on GaN technology. Achievements to date include the following:

- Hosted workshop and produced technology roadmap for inorganic, solid-state lighting. (Funded in part by DOE/BTS.)
- Described the effect of Ga vacancies and N interstitials on hydrogen in GaN.
- Transferred GaN MOCVD growth processes to a new growth reactor.
- Improved sapphire reactive ion etching, which is critical for extending low-defect cantilever epitaxy to larger areas and reducing defects over nucleation mesas.
- Examined important chemical reaction sink processes in AlGaN MOCVD growth.
- Began characterization of gas-flow instabilities using laser-deflection techniques.
- Developed new concept for significantly improved light extraction in LEDs, and began collaboration on realization of visible photonic lattices in LEDs.
- Improved some important components (p-type contacts, stress control for distributed Bragg reflectors, etc.) for UV LEDs and VCSELs.
- Characterized a tri-phosphor blend using commercial inorganic phosphors for near-UV excitation and with good color rendering.

These accomplishments represent significant progress in the few months since this project's inception.

Increased Funding Request

In order to meet the tremendous opportunities in solid-state lighting and in GaN materials, we are submitting a continuation proposal for $2.3M. This is in keeping with the finding of the EAC committee that the project at present has insufficient resources to accomplish its stated tasks. With the increased funding we intend to intensify our efforts by devoting additional man-hours to achieving our milestones. In particular, we plan to develop a stronger device research component. Since our growth chemistry and reactor modeling efforts are already world leaders, additional emphasis on device research will enable us to demonstrate leadership in solid-state lighting as a whole. Also, the larger program will allow us to expand the project to include other areas where Sandia has some particular strengths – e.g., packaging of LEDs for high-temperature and UV (John Emerson); failure analysis and reliability testing (Dan Barton); and integration of intelligence (e.g., microsystems and MEMS) into lighting where solid-state lighting may offer some new unique value for lighting (e.g., the *smart luminaire*).

In the following sections we give detailed reports on our accomplishments during the past year and on the work we have planned for FY02.

ACCOMPLISHMENTS

The tasks have been restructured since the original proposal to provide a tighter programmatic focus and to reflect guidance from the External Advisory Committee.

1 NITRIDE MATERIALS OPTIMIZATION

1.1. GaN Materials Characterization and Theory

The goal of this task is to develop a fundamental understanding of the material characteristics of (In,Al)GaN materials. These materials are quite different from other III-V compounds semiconductors, and a fundamental understanding will be required to minimize the effect of defects, optimize device structures for maximum performance, and to obtain controllable material properties (e.g., doping). The task uses a combination of theoretical calculations and defect characterization (DLTS).

We have performed density-functional-theory calculations for the atomic structures, formation energies, and defect energy levels of gallium vacancies (V_{Ga}) and nitrogen interstitials (N_I) in GaN. V_{Ga} produces singlet and doublet levels centered 0.3 eV above the valence-band maximum and separated by 0.1 eV. The singlet falls below the doublet and is fully occupied in the neutral charge state. The doublet is occupied by one electron in the neutral charge state, thereby allowing V_{Ga} to act as a deep triple acceptor in *n*-type GaN. N_I is predicted to adopt one of two distinct structures depending on the Fermi level. In *n*-type GaN, N_I is predicted to reside in the center of a *c*-axis channel. This structure produces a singlet level near the valence-band maximum containing two electrons in the neutral charge state and a doublet level roughly 1.5 eV above the valence-band maximum occupied by one electron in the neutral charge state. As a result, N_I behaves as a deep triple acceptor in *n*-type GaN, similar to V_{Ga}. In undoped and *p*-type GaN, N_I shares a lattice site with an existing nitrogen atom forming a split-interstitial configuration. This structure produces two singlet levels roughly 0.3 and 1.1 eV above the valence-band maximum. The lower level is occupied by two electrons in the neutral charge state and the upper level contains one electron in the neutral charge state. N_I can therefore act like a single acceptor in undoped GaN or a triple donor in *p*-type GaN. A notable difference between V_{Ga} and N_I is that the formation energies for N_I are higher. N_I is therefore not expected to incorporate significantly into GaN during growth. (It will be produced during ion implantation, however, and may co-incorporate with hydrogen during growth.) V_{Ga}, on the other hand, is predicted to readily incorporate during the growth of *n*-type material where it compensates the Si dopants. The interaction of hydrogen with V_{Ga} and N_I has been studied. Hydrogen can either compensate these defects by transferring an electron to a defect acceptor level, or passivate the defect by forming a hydrogen-defect complex. Removal energies for these hydrogen-defect complexes were computed as a function of the Fermi level and the number of hydrogen atoms in the complex. The removal energy (and therefore the stability of the complex) was found to depend strongly on Fermi level.

These results will be reported in the following two journal submissions:

1. *Interaction of hydrogen with gallium vacancies in wurtzite GaN*, A. F. Wright, J. of Appl. Phys. submitted.
2. *Interaction of hydrogen with nitrogen interstitials in wurtzite GaN*, A. F. Wright, J. of Appl. Phys. submitted.

DLTS measurements of GaN samples will commence next quarter.

1.2 Low-defect Epitaxial Growth and Substrates

The thermodynamic properties of GaN favors bulk crystal growth at exceptionally high temperatures and pressures, with the net result that bulk GaN crystals suitable for wafering into substrates have yet to be produced. The result is that all GaN work to date has used hetero-epitaxial growth on substrates with large mismatches in lattice constant and thermal expansion coefficients. A critical element for improving device performance and yield is the development of epitaxial growth techniques with low defect densities.

We developed and patented prior to the initiation of this project a new low-defect GaN epitaxial growth technique ("cantilever epitaxy"). GaN cantilever epitaxy reduces the defect density by two orders of magnitude (i.e., around $10^7/cm^2$) compared to GaN growth on sapphire substrates (defect densities between 10^8 and $10^{10}/cm^2$).

Cantilever epitaxy (CE) is a simpler approach compared to other low-defect epitaxial growth methods because it uses only a single epitaxial growth. The technique starts with forming μm-scale support mesas in sapphire (or potentially other substrate materials). A single, temperature-varied nitride growth sequence laterally grows low-defect GaN from the support mesa. The growth process begins with growth of a standard low-temperature nucleation layer on the previously patterned substrate. This is followed by a limited growth of GaN (≥0.4 μm) at high temperature to produce a coalesced, smooth surface and GaN sidewalls from which to initiate rapid lateral growth. The temperature is then increased to produce more rapid lateral growth than vertical growth. Cantilevers grow laterally from the side surfaces of the GaN that grew during the first high-temperature phase. To achieve a continuous GaN surface, the cantilevers are grown to coalescence. This process results in cantilevers with very few threading dislocations (TDs$<10^7/cm^2$).

Initial work has showing significant progress in reducing dislocation in both the cantilever surface and the coalescence front. Figure 1.1 presents an SEM image showing four and a half cantilever spans (2.2 μm thick), each 8.4 μm wide, over a 2.1-μm-deep trench, suspended between 2.8-μm supports. Both the top and bottom surfaces of the cantilever are essentially flat with the cantilever tilt being ≤ 0.1 º, as determined by atomic force microscopy (AFM). Although a notch is present at the lower interface of two converging cantilevers just after coalescence (Fig 1.2), the notch is absent in this thicker growth. A significant portion of the coalescence front in CE appears to be free of TDs, as observed by cross-section TEM (Fig 1.2) on the barely coalesced samples. Various ratios of trenches/mesa have been demonstrated. (Fig 1.3).

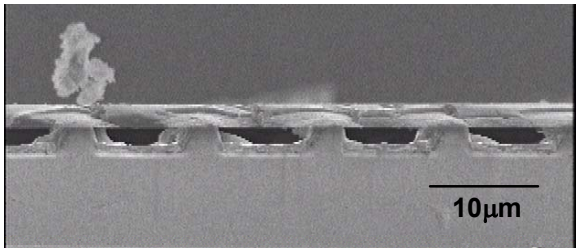

Figure 1.1. SEM micrograph of cantilever epitaxy.

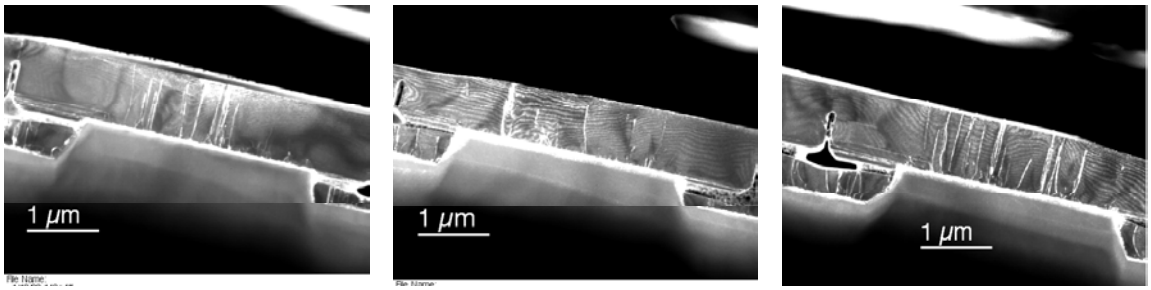

Figure 1.2: Cross-section TEMs of cantilever epitaxy

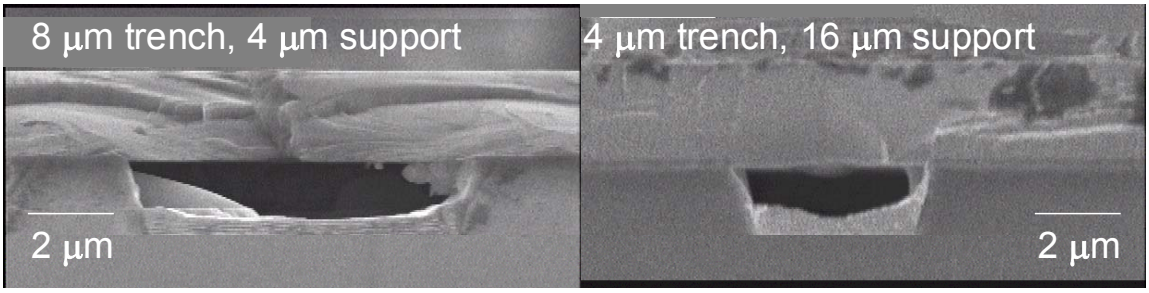

Figure 1.3. Different support and trench sizes in CE.

These initial results were obtained from sapphire wafers that were etched using a BCl_3-based plasma in an inductively coupled plasma reactor where the trenches were approximately 2μm deep and the mesas were approximately 2μm in width. The aspect ratio of the mesa width and trench depth limits the vertical growth that can be done before filling in the trench and interfering with the cantilever growth. For this aspect ratio, the vertical growth over the mesa must be terminated before all the dislocations in this region have a chance to interact and annihilate. This leaves a region over the mesa where dislocations continue to propagate. Dislocation theory suggests that we can eliminate dislocations over the mesa too if sufficient vertical growth is achieved. Hence improvements in the aspect ratio (i.e. reduce mesa width for the same etch depth) could lead us to a lower dislocation density even over the mesa region, and consequently, over the entire wafer.

To test this theory, process development of the sapphire etch has been done to establish mesa widths of 1um or less while maintaining > 1um etch depth. These aspect ratios and critical dimensions have now been demonstrated in sapphire wafers (Fig 1.4b). This has also been achieved over large areas (regions of approx. ¼ of a 2-inch diameter wafer) that are more than sufficient for devices. This is another significant step forward as attempts to integrate devices on sapphire etched using the previous process failed due to highly non-uniform etching of the sapphire.

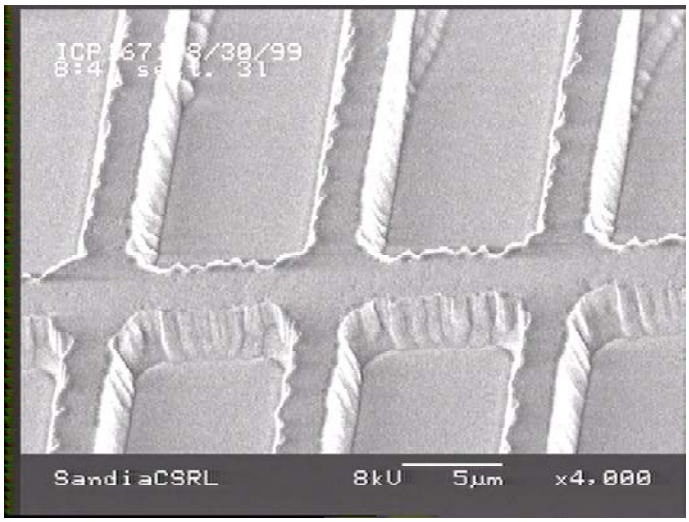

(A)

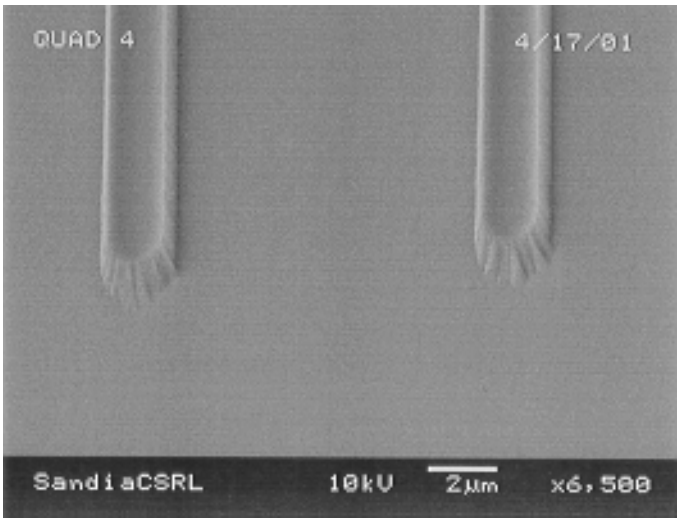

(B)

Figure 1.4 SEM photomicrographs of previous (A) and improved (B) mesas etched in sapphire.

2. III-NITRIDE GROWTH AND REACTOR DESIGN

III-nitride MOCVD growth does not follow the typical MOCVD growth behavior of other III-V material systems and has proven to be more difficult to control. Improvement of material quality (i.e., device performance) and yield (i.e., production cost) will require improved understanding of nitride MOCVD. This task examines the fundamental

chemistry, in-situ process monitors and controls, and optimized reactor design for nitride MOCVD.

2.1 III-Nitride MOCVD Chemistry

Previous Sandia results (J. Han) measuring the GaN and AlN deposition rate as a function of the total reactor pressure gave us clear and compelling evidence that a "parasitic" or "sink" process does exist under normal operating conditions. The "parasitic" process leads to a reduction in the growth rate from the mass-transport limit, and also leads to a very non-linear Al+Ga alloy composition dependence in most nitride CVD reactors. The reduction in growth rate and the non-linear alloy response are two problems severely impacting the cost and quality of AlGaN material.

While the experiment varying total pressure was instructive, it told us very little about the chemical nature of the "parasitic" chemistry because a variety of chemical mechanisms could explain the result. We have therefore expanded the experiments to include conditions that accentuate the differences in proposed "parasitic" chemical mechanisms. Since AlN exhibits the highest degree of "parasitic" chemistry, we have initially focused on this material. We have found that as the tri-methyl aluminum (TMAl) concentration is varied the deposition rate responds in a sublinear fashion and eventually saturates. This behavior is rather unique, and is totally incompatible with a unimolecular "parasitic" term, which would still exhibit a growth rate linear in TMAl. Instead, this behavior can be modeled quantitatively using bimolecular chemical reactions in the loss mechanism, e.g. 2TMAl $\rightarrow$ inactive product.

Perhaps the most important question deals with the thermal requirements of the "parasitic" chemistry. Does the "parasitic" pathway turn on at low temperatures (e.g. near the inlet), or does it only happen when the gases get very hot (e.g. near the wafer)? Much of the folklore regarding reactor design issues for AlGaN CVD revolves around this issue. We combined a simple bimolecular kinetic model with the RDR scaling relationships into a "back-of-the-envelope" calculation and found that varying the total reactor flow rate could differentiate the two extreme scenarios (cold gas vs. hot gas "sink" terms). This difference occurs because the reactor residence time and the boundary layer residence time respond differently to changes in total flow rate. Recent SPIN calculations verify the overall trend, and will allow for a more quantitative comparison with our new experiments.

The experiment involved growing AlN at the matched flow condition (F_m) and 2 X F_m (achieved by increasing the H_2 and NH_3 flow in concert with all other reactor controls kept constant). For ideal CVD systems, e.g. GaAs, the deposition rate under transport limited conditions drops almost exactly in half at F_t = 2 X F_m , simply due to dilution effects (tested experimentally and verified with SPIN). In a system with a parasitic sink term the deposition rate may actually increase as F_t is increased, despite the decrease in precursor concentration, because of the reduction in residence time. For our RDR AlN conditions, SPIN predicts a 44% increase in the deposition rate at 2 X F_m for the "cold-gas" mechanism, and a 2% increase for the "hot-gas" mechanism. Experimentally we observed an increase of 10 ± 5%, which is more indicative of the "hot-gas" mechanism. Thus, it appears that for AlN the parasitic chemical reactions occur mainly in the hot boundary layer near the surface. This conclusion is also supported by our FTIR and

mass spectroscopy results that have failed to find any evidence for a low-temperature "parasitic" mechanism. In the future we plan to refine the total flow rate experiments (e.g. account for temperature drifts) and examine the spin rate dependence, while comparing the results with SPIN calculations.

We have also begun working on an MPSalsa model of our RDR with chemistry, in order to test for finite size effects in the growth rates and uniformity. Initial results using our simple chemical model exhibit a deposition rate that is ~10% higher at the wafer edge, which is in qualitative agreement with experiment.

We presented some of our initial research on AlGaN chemistry at a workshop ("Low Temperature Nitride Precursor Reactions", J.R. Creighton, Tenth Biennial Workshop on Organometallic Vapor Phase Epitaxy, March 11-15, San Diego CA, 2001).

2.2 In-situ Process Controls

Previous pyrometry probes for temperature measurement were designed for use with opaque substrates, so these techniques will need to be re-examined for use with GaN MOCVD. Optical probes capable of emissivity-correcting pyrometry have been installed on both of Sandia's active GaN reactors. A new software package, Thermogrow, has been completed and is used to take data with the new optical probes. Thermogrow can simultaneously record reflectance and thermal emission at two different wavelengths, allowing one to measure at low (500°C) and high (1050°C) temperature conditions. We will determine whether the errors associated with transparent substrates are severe enough to disqualify this technique as a practical temperature measurement tool.

We are also testing a system that performs direct pyrometry using a wavelength above the GaN bandgap, ensuring an opaque substrate, and exploring a suggestion by Art Fischer to measure the temperature-dependent phosphorescence from Cr^{+3} impurities in sapphire as a novel way to obtain the wafer temperature.

We presented our recent research on improvement of in-situ temperature measurement using pyrometry ("Emissivity-Correcting Pyrometry for OMVPE Applications", W. G. Breiland, L. A. Bruskas, A. A. Allerman, and T. W. Hargett, Tenth Biennial Workshop on Organometallic Vapor Phase Epitaxy, 11-15 Mar 2001, San Diego, CA).

2.3 Reactor Design and Modeling

Beam-deflection Measurements of Flow Instability

Flow instability is a fundamental characteristic of any system, but it may be a larger issue for GaN MOCVD growth due to the high growth temperatures and pressures. We have set up and tested a beam deflection (mirage-effect) experiment to make non-invasive measurements of flow instabilities in a rotating disk reactor. These experiments are designed to test our understanding of the factors that lead to chaotic flow during CVD. Theory predicts that the boundary between stable and unstable flow is described with a simple dimensionless number (mixed Rayleigh number). The experiment measures the vertical deflection of a laser beam that is passed over the surface of the disk. Temperature gradients in the gas cause a deflection of the beam, and instabilities cause the deflection to become time-dependent. Figure 2.1 shows a vertical profile of the laser

beam under four flow conditions. Each profile is labeled with the disk temperature, the disk spin rate, and the RMS deviation of the beam mean, averaged over 100s. All high-temperature conditions yield fluctuations that are at least 40 times less stable than the room temperature value. As the disk is spun at faster rates, the temperature gradient becomes sharper and the beam is deflected more. Apparent "noise" on the room temperature profile is actually diffraction fringes caused by the bottom of the laser beam hitting the front edge of the disk. These fringes may be modeled with Kirchhoff diffraction theory to extract a precise position of the center of the laser beam above the disk.

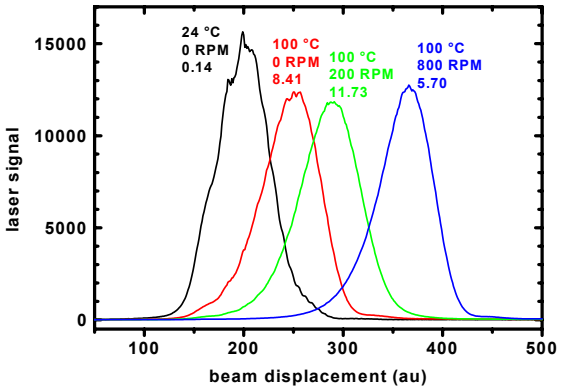

Figure 2.1. Laser deflection experiment.

Reactor Modeling and Optimization

To allow scale-up and optimization of GaN reactors, detailed models of the coupled fluid mechanics and CVD chemistry are needed. We have completed the first stage of this process by setting up the computational infrastructure to allow us to perform optimization operations on model results generated by Sandia's MPSalsa code. Objective functions that measure deposited film non-uniformity and reactant efficiency have been constructed along with an ability to displace mesh variables to accommodate optimization of inlet geometries. A very simple chemistry was chosen to make checking other results from the optimization easier to verify. As we learn more about the chemical mechanisms of GaN and AlGaN growth, more realistic mechanisms will be added. We are currently comparing the predicted thin film uniformity with experimental results for GaN films.

An optical method (CARIS technique) using the reflectance spectrum of a single GaN film was used to measure the thickness profiles (Fig. 2.2). The uniformity of run cv2058 is consistent with predictions from the MPSalsa code. However, an "identical" run, nf1120a, yielded grossly non-uniform results. The reactor inlet underwent slight changes between these two runs. These results clearly point out the need to thoroughly understand the CVD chemistry and to construct robust inlets that do not exhibit such severe run-to-run discrepancies.

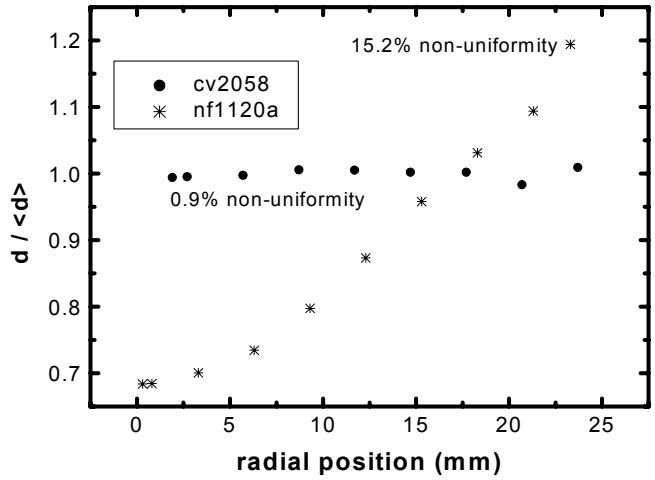

Figure 2.2. Deposition uniformity from two growths using slightly different inlet geometries.

3. SOLID-STATE LIGHTING DEVICES

This task examines improvement of solid-state lighting devices across the visible spectrum. The goal of the National Initiative in Solid-State Lighting is to obtain a solid-state white-light source with good color rendering and an efficacy above 100 lumens/W, which will require improvement of visible and near-UV light emitters and of luminescent materials.

3.1 Light Extraction in LEDs

Light extraction is one of the oldest problems in LED literature. The problem is due to the high refractive index (over 3) of most semiconductors, which causes most of the light (>95%) to be internally trapped due to total internal reflection. While a large number of options have been examined, the best external quantum efficiency reported to date for a visible LED is only around 55% while the theoretical maximum is 100%.

The approaches to enhancing light extraction may be divided into geometrical (structures large relative to the wavelength) and photonic (structures on the order of or smaller than the wavelength) approaches.

Micro-emitter Arrays

We describe a new approach that has the performance of a hemispherical dome (potentially 100% extraction efficiency), uses planar processing common to the semiconductor industry for manufacturability, and is scaleable to larger sized LEDs. The key feature of the new approach is the division of a large-area LED into an array of much smaller emitters (“micro-emitter array”). Each emitter has an integrated optical element to enhance the extraction of light. The optics required for extracting light from the LED scales with the dimensions of the LED. Therefore, the integrated optical elements are now small enough that they can be fabricated with planar processing techniques that are common in the semiconductor industry. Micro-optics are used for a variety of optical

applications and are commercially available; many of the fabrication techniques from the micro-optical industry (e.g., "gray-scale" lithography) could be used for fabrication of integrated optical elements. The concept is illustrated in Figure 3.1.

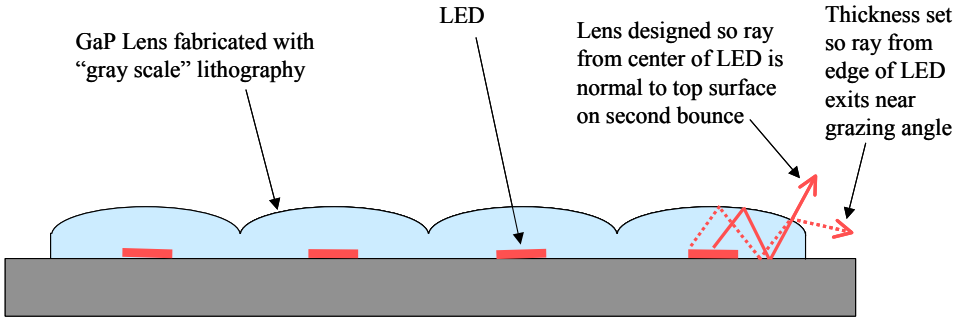

Figure 3.1. Illustration (cross section) of micro-emitter array concept with integrated optical elements for light extraction. The LED is on the order of 1 to 4 μm wide while the optical element is on the order of 5 to 20 μm thick. The optical element is typically the same semiconductor used for the cladding layer in the LED. GaP is shown in the illustration. GaP is commonly used as the cladding layer for AlInGaP alloys, which are used for red- and yellow-emitting diodes. GaN could also be used for the optical element. GaN is commonly used as the cladding layer for AlInGaN alloys, which are used for UV-, blue-, and green-emitting diodes.

Hemispherical domes could have nearly 100% extraction efficiency since all rays from the LED at the center of the hemisphere will be nearly normal to the surface. Other shapes can also be used. The advantage of other shapes is to reduce either the thickness of the optical element for easier fabrication and reduced semiconductor volume (i.e., reduced cost), or to reduce the spacing of the optical elements (greater density of emitters would have higher brightness). Figure 3.2 provides an example geometry. These alternative approaches require a reflective rear surface and have a longer internal path length, which provides opportunity for optical losses.

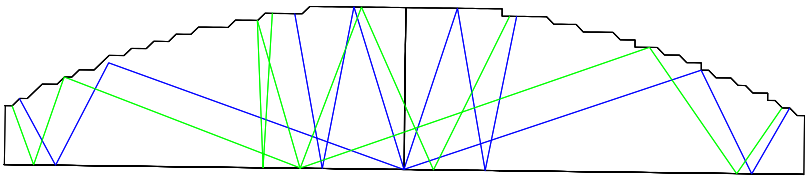

Figure 3.2. Example of non-spherical geometry that reduces volume of optical element by factor of 4 compared to a hemispherical dome. Some representative rays from the LED are shown to illustrate how they are extracted from the optical element.

A Technical Advance disclosure was filed on this concept. We have also begun examination of a closely related concept (array of shaped micro-emitters) that should be much easier to fabricate.

Photonic Crystals

The simplest photonic structure uses distributed Bragg reflectors to enhance light extraction in the vertical direction. These structures include resonant-cavity LEDs and VCSELs, and are discussed in the next section.

Photonic crystals use a periodic modulation of the optical properties in 2 or 3 dimensions to affect the photonic density of states. These structures can be designed to eliminate or to efficiently extract lateral modes. The technical issues include: best design for light extraction, realization of photonic lattices at optical wavelengths, and compatibility of the photonic lattice with the device properties of the semiconductor light emitter.

We have begun modifying our optical models to examine photonic crystals for enhancing light extraction in LEDs. We have also begun a collaboration with an industrial partner (Lumileds) to demonstrate a photonic crystal in an LED.

3.2 UV LEDs & VCSELs

Progress on UV LEDs and VCSELs has advanced on several fronts, both in device processing and in understanding the mechanisms of stress engineering of extreme wide bandgap nitrides. Device processing improvements include an order of magnitude reduction in the transparent p-contact resistance through the development of superior surface treatments. Figure 3.3 shows transfer length method (TLM) data for Ni/Au contacts deposited on p-type GaN demonstrating a specific contact resistivity of 3×10^{-3} Ω cm^2. Studies of the dependence of the thickness of the transparent p-contact on transmission and resistivity are in progress. Studies of the light emission from a new LED structure fabricated on double-side polished (DSP) sapphire have elucidated the fact that the bottom emission is significant, and is otherwise lost in our current processing and measurement scheme. As shown in Fig. 3.4, it was found that coating the backside of the wafer with a highly reflective aluminum mirror produced a more than two-fold increase in the output power of an LED operating at 410 nm. A new mask set has been designed that will allow the study of current crowding, diode size effects, and enable more processing diagnostics that can be evaluated for each diode run, which will improve processing quality and efficiency.

Currently, UV LED structures are grown on top of a 3-micron GaN template that acts as a pseudosubstrate for subsequent device growth. It has been found empirically that this is necessary in order to circumvent the lack of a suitable lattice-matched substrate and produce the highest quality crystal structures; however, this is problematic for UV emitters in that this thick GaN layer is highly absorbing for wavelengths shorter than 360 nm. In order to overcome this challenge, we have begun to design bottom-emitting structures with AlGaN psuedosubstrates and resonant cavity structures that employ distributed Bragg reflectors (DBRs) between the GaN pseudosubstrate and the active region to minimize or eliminate absorptive losses from the pseudosubstrate.

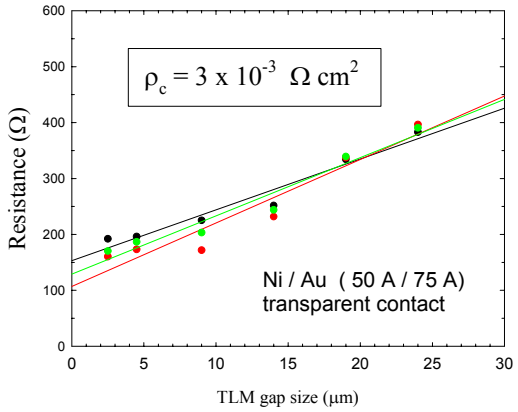

Figure 3.3. TLM data for Ni/Au (50/75Å) contacts on p-type GaN.

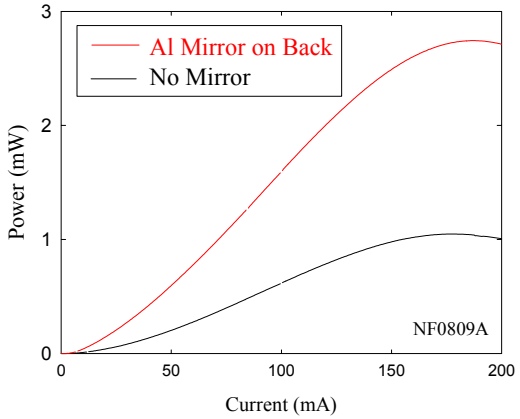

Figure 3.4. Light versus current curves for an LED emitting at 410 nm. Note the dramatic increase in output power for devices with an Al mirror on the back surface.

The stress engineering challenges associated with the employment of bottom DBRs for UV LEDs is also critical to the UV VCSEL effort. Stress control in the thick, highly strained UV Bragg reflectors relies on the use of AlGaN-based interlayers. Investigations into the morphology and defect structure of the interlayers are in progress in order to optimize the mechanical, optical, and electrical benefits of the interlayers for UV optoelectronics. It has been found that the interlayers do not adversely affect the reflectivity of the mirrors, and can prevent cracking. As shown in Fig. 3.5, we have learned that AlN interlayers deposited at high temperature (1050°C) are not continuous films and show non-coalesced islands of material. Although the optimum interlayer structure is not known at this time, it is thought that these islands may be required to relieve the strain built up in multi-layer GaN/AlGaN DBRs.

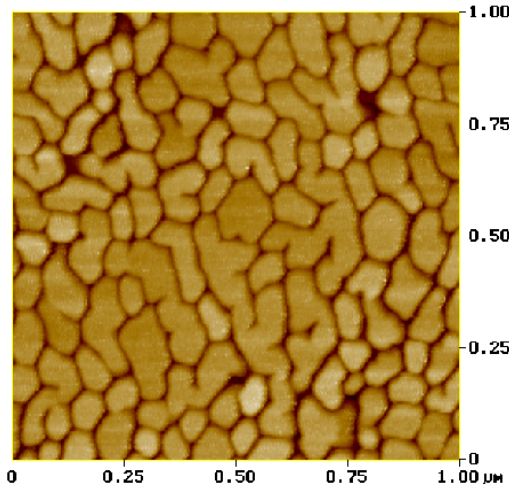

Figure 3.5. AFM image of a 135 Å HT-AlN interlayer.

Finally, our UV dielectric mirror capability, which will be used in VCSEL and resonant-cavity LED designs, has improved considerably. Figure 3.6 shows data from a hafnium dioxide/silicon dioxide Bragg reflector with greater than 98% reflectivity, which was deposited in an electron-beam evaporator. This particular evaporator is designed to evaporate metals, and we have found that this tool is not ideal for careful control of dielectric processes. We are seeking alternative deposition methods for better control and properties of the in-house production of dielectric Bragg reflectors for 300-400 nm.

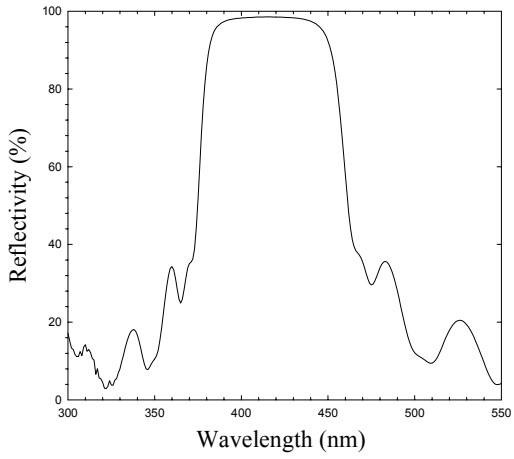

Fig. 3.6 Reflection spectrum from a 23-layer HfO_2/SiO_2 dielectric mirror.

3.3 Luminescent Materials

Many approaches exist for generating white light using solid state devices, e.g., multi-chip LEDs; blue LED + yellow phosphor; blue LED + green and red phosphors; and UVLED + red, green, and blue phosphors. An investigation of the latter two approaches is the focus of the Luminescent Materials subtask. We evaluated conventional inorganic phosphors, and will begin evaluation of II-VI semiconductor nanocrystals at excitation wavelengths of 370-460 nm.

A xenon lamp, monochromator, and spectroradiometer were used to obtain preliminary photoluminescence data for conventional red, green, and blue-emitting phosphors in the 370-420 nm range. Next, triphosphor blends were fabricated using the phosphors with the highest luminous output at the wavelength of interest. Color rendering index (R_a) was calculated for each blend. Figure 1 shows the emission spectrum of a triphosphor blend with good color rendering index (R_a) consisting of $Y_2O_2S:Eu^{3+}$ (red-emitting), ZnS:Cu,Al (green-emitting), and $BaMg_2Al_{16}O_{27}:Eu^{2+}$ (blue-emitting) under xenon excitation at 370, 380, 385, and 390 nm.

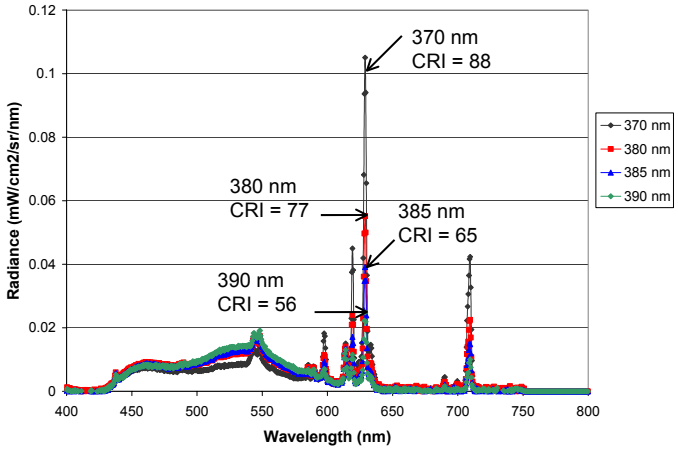

Figure 3.7. Radiance ($\mu W/cm^2/sr/nm$) as a function of wavelength (nm) for a triphosphor blend candidate for UVLEDs. Xenon lamp excitation at 370, 380, 385, and 390 nm.

As shown in Figure 3.7, color rendition is highest at an excitation wavelength of 370 nm and decreases as the excitation moves towards the visible region. This is due to the less than optimal absorption of the red component of the blend, $Y_2O_2S:Eu^{+3}$ in the near-UV. Our preliminary evaluation has determined that a few conventional phosphors are excitable in the NUV-visible range, as listed in Table 3.1.

Table 3.1. Conventional inorganic phosphors excitable in the NUV-VIS (370-420 nm).

Phosphor	Color	Emission peak (nm)
$BaMg_2Al_{16}O_{27}:Eu^{2+}$	Blue	452
$Sr_{10}(PO_4)_6Cl:Eu^{2+}$	Blue	447
ZnS:Cu,Al	Green	540
$SrGa_2S_4:Eu^{2+}$	Green	538
$Y_2O_2S:Eu^{3+}$	Red	630

Note that even though these phosphors are excitable in the NUV-visible, their luminous output is not optimized for operation at these wavelengths. There are techniques involving activator sensitization that can be utilized to optimize these materials over the wavelength range of interest for LEDs.

The focus of this subtask will shift towards the characterization of II-VI nanocrystals as alternative materials to conventional phosphors in the NUV-visible regime. The synthesis of nanocrystals of CdS, CdSe, and CdTe is currently in progress. We currently have 1-2 nm diameter CdSe nanocrystals with a peak emission wavelength of 500 nm under 420 nm excitation. Synthesis of larger, red-emitting, CdSe is being investigated, as well as CdTe. An important technical challenge will be stabilization of these nanocrystals in a matrix suitable for LED packaging. When available, the samples will be evaporated for initial characterization.

4. SMART LUMINAIRE

No work was conducted in this task due to limited resources.

WORK PLANNED

During the next year, we plan to secure Sandia a stronger reputation in solid-state lighting with a goal of positioning ourselves for a leadership position in any new National Initiative. This will require the integration of our material science, low-defect epitaxy, and MOCVD chemistry tasks to produce improved devices. Specifically, we will:

- Initiate experimental characterization (DLTS) of defects in GaN. Compare experimental results with other characterization techniques and with theoretical calculations. Further refine numerical simulation tools (e.g., implement the GW technique within the Projector-Augmented Wave formalism) in order to get more accurate defect energy levels.
- Refine cantilever epitaxy and stress management during MOCVD growth for large-area low-defect ($<10^7/cm^2$) substrates. This will include: complete optimization of high-aspect ratio etching of sapphire for more optimal growth geometries; optimize growth process on these 2nd generation patterned sapphire wafers; establish mechanical and optical properties of cantilever epitaxial films; and compare LED performance on CE and typical GaN buffers.
- Refine AlInGaN MOCVD chemistry models.
- Demonstrate improved in-situ temperature measurement in GaN MOCVD.
- Demonstrate improved fully coupled reactor modeling.
- Demonstrate improved light extraction in an LED using micro-emitter array.
- Demonstrate a visible photonic lattice for improved light extraction.
- Demonstrate components for high-efficiency VCSELs (electrical conductivity with distributed Bragg reflectors, current apertures, etc.). Demonstrate conventional and resonant-cavity UV LEDs using improved components, stress engineering, and low defect substrates.
- Further explore white light source using UV and/or blue LEDs and semiconductor quantum dot-based luminescence. Issues include fabrication of semiconductor nanocrystals with appropriate excitation bands and luminescent wavelengths, and stabilization of nanocrystals in suitable medium for encapsulation in LED package.

- Develop concept for a *smart luminaire*, and initiate UV LED/VCSEL packaging research. Specific packaging research challenges that might be addressed include: encapsulation for high-flux UV/blue transmission and high die temperatures (>100°C), die attach materials, thermal management, precision alignment of devices, and color mixing optics.

SIGNATURES

Principal Investigator:

_____

James Gee, 06201

Project Manager:

_____

Jerry Simmons, 01123